Resonances in $\bar{\nu}_e - e^-$ scattering below a TeV

Vedran Brdar[1,2,*] André de Gouvêa[1,†] Pedro A. N. Machado[2,‡] and Ryan Plestid[3,2,§]

[1]*Northwestern University, Department of Physics and Astronomy,*
2145 Sheridan Road, Evanston, Illinois 60208, USA
[2]*Theoretical Physics Department, Fermilab, P.O. Box 500, Batavia, Illinois 60510, USA*
[3]*Department of Physics and Astronomy, University of Kentucky, Lexington, Kentucky 40506, USA*

We consider the resonant production and detection of charged mesons in existing and near-future neutrino scattering experiments with $E_\nu \lesssim 1$ TeV, characteristic of high-energy atmospheric neutrinos or collider-sourced neutrino beams. The most promising candidate is the reaction $\bar{\nu}_e e^- \to \rho^- \to \pi^- \pi^0$. We discuss detection prospects at FASERν, the LHC's forward physics facility with nuclear emulsion (FASERν2) and liquid argon detectors (FLArE), and we estimate the number of expected resonance-mediated events in the existing data set of IceCube. We also outline possible detection strategies for the different experimental environments. We predict dozens of events at the forward physics facility and identify cuts with order-one signal efficiency that could potentially suppress backgrounds at FASERν, yielding a signal-to-background ratio larger than 1. Antineutrino-induced s-channel meson resonances are yet unobserved Standard Model scattering processes which offer a realistic target for near-term experiments.

I. INTRODUCTION

Resonances are among the most distinctive and historically important observables in particle physics. In particular, s-channel resonances imprint the unmistakable signature of on-shell particles onto experimental data. Famous examples include the discovery of the J/ψ meson [1,2], the Z boson [3–5], and the Higgs boson [6,7].

Relative to the rest of particle physics, resonances have played a minor role in the history of neutrino scattering physics. Typical experimental configurations aim neutrino beams at detectors composed of electrons and nucleons. Since neutrinos carry lepton number, the only relevant Standard Model (SM) s-channel reaction is $\bar{\nu}_e e^- \to R^-$ where R^- is a charged state with zero baryon and lepton number. The canonical example is the Glashow resonance $\bar{\nu}_e e^- \to W^-$ [8], which was recently identified as the likely origin of one candidate event in the IceCube neutrino observatory [9]. The production of W bosons from antineutrinos scattering on electrons at rest requires ultra-high energies, $E_\nu = M_W^2 / 2m_e = 6.3$ PeV. As no terrestrial

sources of neutrinos can reach such high energies, only the highest energy astrophysical neutrinos can produce a Glashow resonance.

A natural question is whether neutrino beams can be used to produce observable resonances at lower energies. Of particular interest are neutrinos from the LHC and the associated forward physics facility (FPF) [10]. For $E_\nu \lesssim 1$ TeV, $s = 2m_e E_\nu <$ few GeV^2 charged resonances around or below the GeV scale, carrying neither baryon nor lepton number, are, in principle, accessible. These are the light (and, perhaps, charmed) charged mesons. The idea of detecting the ρ^--meson resonance at IceCube was first sketched in [11]. More recently, neutral meson resonances were considered in the context of the cosmic neutrino background [12].

In this paper we consider the production of charged mesons $\mathfrak{m}$ via $\bar{\nu}_e e^- \to \mathfrak{m}$; these may be considered the low-energy analogs of the Glashow resonance (see Fig. 1). From the perspective of neutrino physics, these events are interesting because they potentially provide event-by-event flavor tagging and because of their unique event topology. In particular, $\bar{\nu}_e e^- \to \mathfrak{m}$ is expected to "look" very different from the more abundant deep inelastic scattering (DIS) process. We estimate the number of resonant events in FASERν [13], FLArE [14], and IceCube [15]. We further discuss event topologies in Cherenkov, nuclear emulsion, and liquid argon time projection chamber (LArTPC) detectors, outlining distinctive signal characteristics and potential strategies for suppressing backgrounds, and we comment on the prospect of measuring meson resonances in near-term neutrino experiments.

*vedran.brdar@northwestern.edu
†degouvea@northwestern.edu
‡pmachado@fnal.gov
§rpl225@g.uky.edu

FIG. 1. Resonant production of a ρ^- meson resulting in a $\pi^-\pi^0$ final state.

FIG. 2. Cross section for vector-meson resonances, $\bar{\nu}_e e^- \to \mathfrak{m} \to$ hadrons. For comparison, the corresponding cross sections for W boson production (inset) and $\bar{\nu}_e e^- \to \bar{\nu}_e e^-$ elastic scattering (red line) are also included.

II. GENERAL THEORY

Within the Breit-Wigner approximation the cross section for $\bar{\nu}_e e^- \to \mathfrak{m} \to X$ is given by [9,16,17]

$$\sigma_{\text{res}} = (2J + 1)8\pi\Gamma^2 \text{Br}_{\text{in}} \text{Br}_{\text{fi}} \frac{s/M^2}{(s - M^2)^2 + M^2\Gamma^2}, \quad (1)$$

where J is the spin of the resonance, $\sqrt{s}$ is the center-of-mass energy, M is the mass of the resonance, Γ is the width of the resonance, $\text{Br}_{\text{in}} = \Gamma(\mathfrak{m} \to \bar{\nu}_e e^-)/\Gamma$, and Br_{fi} is the equivalent expression for the decay of a meson into the final state X. The production of pseudoscalar mesons, e.g. π^- or K^-, is chirality suppressed by a factor m_e^2/M^2 and can therefore be safely neglected [42]. Consequently, the lightest meson with a sizable production cross section is the charged vector ρ^-. Neglecting the electron mass, the decay rate of vector mesons into antineutrinos and electrons is given by

$$\Gamma(\mathfrak{m} \to \bar{\nu}_e e^-) = \frac{G_F^2}{12\pi} f^2 M^3 |V_{\text{CKM}}|^2, \quad (2)$$

where V_{CKM} is the relevant element of the quark mixing matrix, G_F is the Fermi constant, and f is the meson decay constant [18]. We use the values of f listed in [19,20], e.g. $f_{\rho^-} = 0.21$ GeV. Figure 2 depicts the cross sections for the production of different vector-meson resonances computed using Eq. (1), where we set $\text{Br}_{\text{fi}} = 1$, along with the corresponding cross section for on-shell W^- boson production (in the inset) and low-energy $\bar{\nu}_e e^- \to \bar{\nu}_e e^-$ elastic scattering.

We estimate the number of resonance-mediated events, N_{res}, at a given experimental setup:

$$N_{\text{res}} = N_e \int_{\frac{(M-n\Gamma/2)^2}{(2m_e)}}^{\frac{(M+n\Gamma/2)^2}{(2m_e)}} \Phi(E_\nu)\sigma_{\text{res}}(E_\nu)dE_\nu, \quad (3)$$

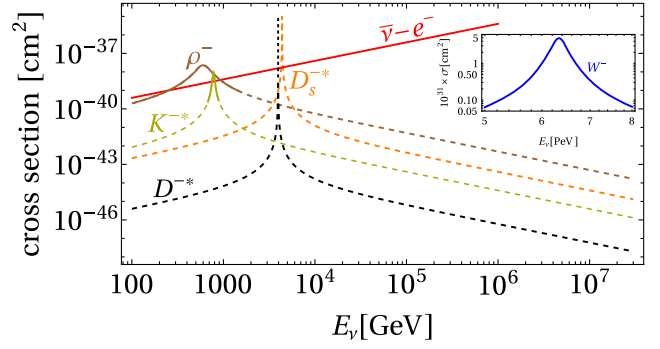where N_e is the number of electrons in the fiducial volume of the detector, Φ is the antineutrino flux, and n denotes the

number of charged meson widths Γ across which the integral is evaluated. For extremely narrow resonances, we checked that our results are equivalent to those obtained using the narrow-width approximation. For the ρ^- resonance, it is well known that the near-peak structure of the resonance deviates substantially from a Breit-Wigner shape. The simplest way to circumvent this difficulty is to calculate $\bar{\nu}_e e^- \to \pi^0\pi^-$ in terms of form factors defined via $\langle \pi^-(k_1)\pi^0(k_2)|V_\mu|0\rangle = (k_1 - k_2)_\mu F_1(q^2) + (k_1 + k_2)_\mu F_2(q^2)$, where $q = k_1 - k_2$ [21,22]. All terms that depend on F_2 are lepton-mass suppressed $O(m_e^2/q^2)$ and can be safely neglected. The form factor F_1 can be extracted from $e^+e^- \to \pi^+\pi^-$ data, but the extraction process requires isospin corrections and the subtraction of the $\omega(782)$ contribution. We instead use a simple isospin-symmetric chiral-perturbation-theory-inspired model with no adjustable parameters; this model agrees with e^+e^- data at the 10% level and explicitly excludes the $\omega(782)$ contribution [23]. Ultimately, this more

TABLE I. Estimated number of ρ^- and K^{-*} resonance-mediated events at different experimental setups. We show results for the cases where the integral in Eq. (3) is within $\pm\Gamma/2$ and $\pm2\Gamma$ of the resonance peak. A dash (–) indicates that less than 0.1 events are expected. For IceCube and DeepCore, we use the effective masses given in Fig. 2 of [24] and consider 10 years of data taking. In parentheses, we indicate the event rates at IceCube and DeepCore for the case when the effective mass matches the total mass. Event rates at present and proposed LHC-based detectors are computed using the fluxes from [25] and the experimental configurations from [26].

Experiment	ρ^-, $\pm\Gamma/2$	ρ^-, $\pm2\Gamma$	K^{-*}, $\pm\Gamma/2$	K^{-*}, $\pm2\Gamma$
FASERν	0.3	0.5	–	–
FASERν2	23	37	0.7	3
FLArE-10	11	19	0.3	2
FLArE-100	63	103	2	8
DeepCore	3 (1)	5 (2)	–	–
IceCube	8 (40)	17 (83)	–	–

detailed procedure yields event rates that are very similar to the ones obtained with Eq. (1), with differences typically below 10%. For obtaining the event numbers in Table I, we employ this improved model for the cross section.

III. THE WEAK R-RATIO

The possibility that $\bar{\nu}_e e^- \to$ hadrons may yield complementary information to $e^+ e^- \to$ hadrons is intriguing. The R-ratio, defined as $R = \sigma(e^+ e^- \to \text{hadrons})/\sigma(e^+ e^- \to \mu^+ \mu^-)$ (see Ref. [27], pages 699–700), is, for example, a key input for estimating the nonperturbative hadronic vacuum polarization [28] and has received increased recent interest in light of the new precision measurements of the $(g - 2)_\mu$ anomaly [29,30]. Given the prominent position occupied by the conventional R-ratio, we are motivated to define its weak interaction analog,

$$R_W = \frac{\sigma(\bar{\nu}_e e^- \to \text{hadrons})}{\sigma(\bar{\nu}_e e^- \to \bar{\nu}_\mu \mu^-)}. \qquad (4)$$

The relevant contributions to R_W are depicted in Fig. 3. For the denominator we take $\sigma(\bar{\nu}_\mu \mu^-) = (96\pi)^{-1} g^4 s \times (M_W^2 - s)^{-2}$, where $s = 2 E_\nu m_e$ and g and M_W are the weak coupling and the W-boson mass, respectively. To compute the numerator of R_W, we focus on resonant energies and use the Breit-Wigner formula [27] with $\text{Br}_{\text{fi}} = 1$ for all mesons depicted in Fig. 3. In addition to the mesonic resonances, we also include the naive constituent-quark-level QCD estimate (dashed gray line), assuming constituent masses of 336 MeV, 340 MeV, and 486 MeV for the up, down, and strange quarks, respectively.

IV. EVENT RATE ESTIMATES

As alluded to in the Introduction, there are two promising sources of neutrinos with $E_\nu \gg 100$ GeV that offer
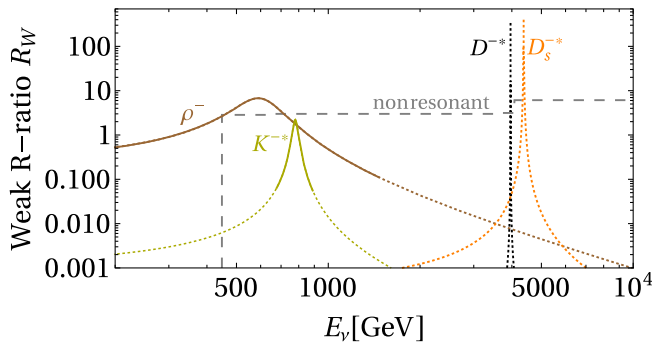
FIG. 3.   Resonant contributions to the R_W cross section ratio, $\sigma(\bar{\nu}_e e^- \to \text{hadrons})/\sigma(\bar{\nu}_e e^- \to \bar{\nu}_\mu \mu^-)$, for different charged mesons. The dashed line depicts the result of a naive perturbative parton-model calculation, with thresholds at the constituent quark masses. For the wider resonances ρ^- and K^{*-}, the region between $E_\nu^\pm = (m \pm 3\Gamma)^2/(2 m_e)$ is drawn with a solid line.

the opportunity to detect meson resonances. First, atmospheric and astrophysical neutrinos offer a broad, steeply falling flux with energies up to the PeV regime. As we argue below, these are sufficiently numerous to produce $O(1)$ events in IceCube per year. Second, neutrinos produced at the LHC offer a high intensity beam with energies ranging from ~ 100 GeV–3 TeV [10], and these neutrinos can be detected using both FASERν [13] and SND@LHC [31]; for our proposed signal SND@LHC does not yield observable event rates, so we focus on FASERν in what follows. We note that FASERν has recently demonstrated the ability to detect and measure neutrino interactions [32]. The planned FPF offers the advantage of high-resolution and larger detectors, including FASERν2's nuclear emulsion detector, and the potential opportunity to deploy a LArTPC further downstream (see Ref. [26] for the FLArE proposal). In Table I, we list the expected number of ρ and K^* resonant events in the aforementioned experiments. IceCube has a subdetector volume with a higher density of digital optical modules that allow for a lower energy threshold and better spatial resolution. This subvolume is referred to as DeepCore [33], and we calculate event rates both for the full IceCube fiducial volume and for DeepCore with both estimates corresponding to 10 years of total exposure. We expect 10–100 ρ^- and 1–10 K^{-*} events in FASERν2 and in the two proposed liquid argon experimental setups, FLArE-10 and FLArE-100. For a comparison, the number of antineutrino-induced D^{-*} and D_s^{-*} resonances is $\sim 10^{-3} - 10^{-2}$. These detectors are envisioned to collect data during the High-Luminosity Large Hadron Collider (HL-LHC) stage [34]; an integrated luminosity of 3000 fb^{-1} is expected for the period 2027–2038.

V. EXPERIMENTAL SIGNATURES

The estimates in Table I do not include the impact of realistic background mitigation strategies. In what follows, we discuss some distinguishing characteristics of resonant meson production and the capabilities of nuclear emulsion, LArTPC, and Cherenkov detectors.

We start with the basic kinematic properties of $\bar{\nu}_e e^-$ scattering and contrast them to DIS, which dominates neutrino-matter scattering for $E_\nu \sim 1$ TeV. At these neutrino energies, to a good approximation, nuclear structure can be neglected, and one can concentrate on neutrino interactions with free nucleons N. The collision is most clearly described in the center-of-mass frame of the νN system, which is connected to the lab frame by the Lorentz factor $\gamma_{\text{cm}} = \sqrt{2 E_\nu / m_N} \sim 36 \sqrt{E_\nu / 600 \text{ GeV}}$. In the center-of-mass frame, both longitudinal and transverse momenta are proportional to $\sqrt{s}$ such that the typical scattering angle in the laboratory frame is $\theta_{\nu N} \sim 1/\gamma_{\text{cm}} \sim 28 \text{ mrad} \times \sqrt{600 \text{ GeV}/E_\nu}$. When antineutrinos scatter on electrons, the boost between the center-of-mass and

laboratory frames is $\gamma_{\rm cm} \sim 1500\sqrt{E_\nu/600\ {\rm GeV}}$, larger by a factor of $\sqrt{m_N/m_e} \sim 43$, resulting in a typical angular scale of $\theta_{\nu e} \sim 0.7\ {\rm mrad}\sqrt{600\ {\rm GeV}/E_\nu}$. Therefore, detectors with mrad angular resolution can easily distinguish between these two different scenarios.

The main resonance-mediated final state for a ρ^- resonance (at $E_\nu \approx 580$ GeV) is $\pi^-\pi^0$, with a branching ratio close to 100%. Interestingly, the system is so boosted that the π^0 is, typically, not prompt: its decay length is $\lambda_{\pi^0} = \gamma\beta c\tau_{\pi^0} \sim (300\ {\rm GeV}/0.135\ {\rm GeV}) \times 25\ {\rm nm} \sim 60\ \mu{\rm m}$, leading to a visible displaced vertex in detectors with spatial resolution of 10 μm or better. The subsequent π^0 decay will result in a $\gamma\gamma$ pair, each of which will convert to an e^+e^- pair in a (typically macroscopic) length scale of order-one radiation length X_0 of the detector material for $E_\gamma \sim 100$ GeV. The conversion lengths of the two photons are realized in stochastic processes such that one photon will convert before the other. Concurrently, the daughter π^- will be ultrarelativistic ($\beta\gamma \gtrsim 1000$) such that radiative energy loss processes dominate over those induced by Bethe-Bloch ionization, and dE/dx can be an order of magnitude larger than that of a minimally ionizing particle.

FASERν is a 1.2 tonne detector located 480 m downstream from the ATLAS interaction point at the LHC; it contains emulsion films and tungsten plates [25]. This kind of detector has a remarkable capability to reconstruct charged tracks and other energy depositions, with spatial resolution as good as 50 nm. FASERν projects a 400 nm spatial resolution, which translates to an angular resolution of 0.06 mrad for track lengths of roughly 1 cm [25]. This allows the detector to identify, e.g., tau leptons, $D^\pm$ mesons, and $B^\pm$ mesons via the "kinks" resulting from their decay inside the detector. The resonant ρ^- signature would consist of a forward track from the π^- and two displaced electromagnetic (EM) showers, coming from the two photons from the π^0 decay (see Fig. 4). The showers would define a vertex slightly displaced from the start of the π^- track. This unique event topology, combined with the absence of other charged tracks, should serve as a powerful veto of DIS events, typically associated with intense hadronic activity.

Furthermore, as discussed above, the typical angle between the π^0 and π^- is of order 0.7 mrad compared to 28 mrad for typical DIS-produced tracks. One can also reconstruct the invariant mass of the $\pi^0\pi^-$ pair and require it to lie within $\Gamma_\rho \sim 150$ MeV of $m_\rho \approx 770$ MeV. Assuming the π^0 and π^- tracks can be reliably identified, their invariant mass is $m_{\pi\pi}^2 = m_{\pi^0}^2 + m_{\pi^-}^2 + E_{\pi^0}E_{\pi^-}\theta_{\pi\pi}^2$, where we are working in the small-angle, ultrarelativistic approximation. Note that E_{π^0} is the reconstructed energy of the $\gamma\gamma$ EM shower, and $\theta_{\pi\pi}$ is the angle between the π^- track and the center of the π^0-induced EM shower. Taking $\delta E/E \sim 5\%/(E/100\ {\rm GeV})^{1/2}$ for both E_{π^-} and E_{π^0} [25,35] and $\delta\theta_{\pi\pi} \sim 10\%$ and assuming that the angular
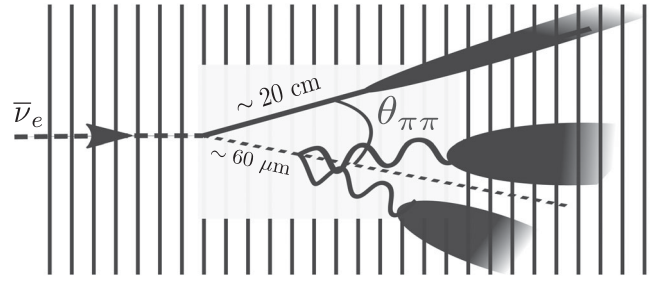

FIG. 4. Cartoon of the typical event topology for $\bar{\nu}_e e^- \to \pi^-\pi^0$ in a nuclear emulsion detector. Two photons (i.e. EM showers) define a vertex displaced by, approximately, 60 μm from a π^- track, which has associated EM activity from hard bremsstrahlung. The showers are displaced by roughly one radiation length from the reconstructed vertex. The opening angle is $\theta_{\pi\pi} \sim m_e/m_\rho \sim 1/1500$.

resolution dominates the error budget [43], we estimate $\delta m_{\pi\pi}^2/m_{\pi\pi}^2 \sim 15\% \times (\delta\theta_{\pi\pi}/10\%)$, which is sufficient to identify the ρ^- peak, even allowing for lower angular resolutions. This measurement can be combined with calorimetric information, which should allow one to reconstruct $E_\nu = m_\rho^2/2m_e \approx 580$ GeV providing two independent criteria with which to identify likely ρ^- candidates.

In addition to the large DIS background which is common across all three experiments, FASERν and FASERν2 must also contend with a large background from through-going muons. The estimates presented in [36] suggest a muon background of 2.5 Hz/cm^2, which translates to 10^5–10^6 muon tracks per cm^2 in a given detector exposure. Our candidate event involves one charged pion track and two displaced electromagnetic showers from $\pi^0 \to \gamma\gamma$. No dedicated studies have been performed that guarantee that this signal can be isolated from the sizable background of electromagnetic showers produced by muons. Nevertheless, future research may reveal new strategies that could enable the isolation of our signal topology from the background, or alternatively, the muon background could be mitigated by using a sweeper magnet as suggested in [10]. In what follows we assume that the muon background can be controlled, and we focus our attention on background events from neutral current DIS.

A ρ^- candidate will have one π^--like track and one π^0-like pair of EM showers, and it can therefore be reduced to three kinematic variables. We take $\omega = E_{\pi^-} + E_{\pi^0}, \theta_{\pi\pi}$, and $m_{\pi\pi}^2$ as a convenient, linearly independent basis. First, we require ω to lie close to 580 GeV. The neutral current DIS cross section is around 100 times larger than the ρ^- production cross section near its resonant peak, and $\bar{\nu}_e, \bar{\nu}_\mu, \nu_e$, and ν_μ all contribute to DIS scattering. Since ν_μ and $\bar{\nu}_\mu$ fluxes are around 10 times larger than those of $\bar{\nu}_e$ and ν_e, we anticipate a signal-to-background ratio of $\sim 1:5000$ imposing only a cut on ω; this is an overestimate

as it ignores particle identification (PID) of the exclusive final state $\pi^-\pi^0$. Next, we require $\theta_{\pi\pi} \lesssim$ few mrad, as this should provide an improvement in the signal-to-background ratio of order $\theta_{\nu N}/\theta_{\nu e} \sim 50$, with a negligible loss in signal events. This cut alone will improve the signal-to-background ratio to $\sim 1:100$ (again neglecting PID). Further cuts may be imposed on charged-track multiplicity and photon multiplicity, as our signal has only one charged pion and two EM showers from the π^0, while typical neutral current DIS events will have much higher hadronic multiplicities. We anticipate a reduction in background by at least 50 (see Fig. 7 of [37]). Finally, we define an additional cut on the reconstructed value of $m_{\pi\pi}$, as defined above, which should agree with the ρ mass to within $\sim 20\%$ accuracy. Naively, this would suppress backgrounds by a further factor of 5; however, $m_{\pi\pi}^2$ is correlated with $E_{\pi^+} + E_{\pi^-}$ and $\theta_{\pi\pi}$, so there is some redundancy in this variable, and the background suppression from such a cut will likely be weaker. Nevertheless, provided this final cut can suppress backgrounds by at least a factor of 2, then a signal-to-background ratio comfortably larger than 1 is achievable, while simultaneously keeping most of the signal events.

The FLArE proposal consists of a LArTPC deployed 620 m from the ATLAS interaction point [26]. While LArTPC detectors do not have the granularity of emulsion detectors, they still have 3 mm spatial resolution, and their calorimetry allows for efficient PID using dE/dx. The radiation length in liquid argon is $X_0 \approx 17$ cm [38], and the angular resolution for a 1 cm track is around 100 mrad [44]. Consequently, the π^- track and the $\gamma\gamma$ pair from the π^0 decay generally overlap. Nevertheless, the track will have a distinct ionization profile. In more detail, for the first 10 cm or so, only the π^- will be visible. Its kinematics, $\beta\gamma \sim 3000$, are such that bremsstrahlung will dominate over ionization; however, the emitted photons will not appear until after a full radiation length, and only the ionization signature will be visible. Further down the track, each γ from the π^0 decay will convert to e^+e^-, each at a different point. In addition to the $\gamma\gamma$ pair from π^0 decay, other hard bremsstrahlung photons produced by the π^- will also pair produce. The result will be a forward-pointing "hadronic flashlight" that has discrete jumps in dE/dx as a function of x with no associated wide-angle hadronic activity from the interaction vertex.

Cherenkov detectors have poorer angular resolution relative to LArTPCs. Therefore, the π^- and the two γs from the π^0 decay will result in a single collimated event. In water, for the energies of interest, the typical hadronic interaction length is $\lambda \sim 90$ cm and the radiation length is $X_0 \sim 30$ cm. Both hadronic and EM cascades are on the order of 5–10 interaction lengths and therefore sufficiently short that the ρ^--mediated events considered here would be classified as "fully contained cascades" in the IceCube nomenclature. This class of events has order 10% energy

resolution, so the ρ^- resonance region, $540\text{ GeV} \lesssim E_\nu \lesssim 640\text{ GeV}$, can be realistically isolated.

Our estimates in Table I suggest that there are around ten resonant $\pi^-\pi^0$ events in IceCube's existing event catalogue, so it is worthwhile to understand if these events can be reliably identified. Typical cascade events involve ν_e or $\bar{\nu}_e$ charged-current scattering or neutral-current events. In both cases the outgoing lepton (electron or neutrino) typically carries away around 80% of the energy while the remaining 20% is transferred to the hadronic system. Concentrating on events where the reconstructed neutrino energy lies inside the ρ^- resonance window, a neutral-current event would need to deposit at least $W_0 \sim 540$ GeV of hadronic energy, corresponding to a typical neutrino energy $E_\nu \sim 2.7$ TeV. Charged-current backgrounds, instead, involve neutrinos with $E_\nu \sim 600$ GeV since both the electron and positron are also fully contained in the cascade. Using the atmospheric neutrino fluxes from [39] and accounting for the energy dependency of the cross sections, we estimate a signal-to-background ratio of order $1:40$ [45] for neutral-current backgrounds and $1:140$ [46] for charged-current backgrounds.

VI. CONCLUSIONS

The production of charged-meson resonances in $\bar{\nu}_e - e$ scattering is an interesting and previously inaccessible SM neutrino reaction. Existing data from IceCube may already hold a handful of ρ^- resonances, but these lie beneath a sizable DIS background. In contrast, the situation at the LHC's FPF appears to be more promising. We estimate 10–100 total meson resonance events at proposed FPF detectors and, while backgrounds are naively also large, their excellent spatial and angular resolutions (in the case of nuclear emulsions) or calorimetry (in the case of LArTPCs) may allow for very effective background rejection while maintaining order-one signal efficiency. It may be interesting to consider the optimal rapidity of an emulsion detector for the purpose of detecting a ρ^- resonance. In [41] the authors note that the spectrum of neutrinos varies with rapidity, and it is conceivable that there exists a detector placement which would supply a flux of neutrinos that peaks at the energy necessary to produce an on-shell ρ^-; however, this lies beyond the scope of the current work. Meson resonances offer an interesting case study that illustrates the capabilities of both nuclear emulsion detectors and LArTPCs and can serve as an intriguing physics target for the LHC's FPF.

---

[1] J. E. Augustin *et al.* (SLAC-SP-017 Collaboration), Phys. Rev. Lett. **33,** 1406 (1974).

[2] J. J. Aubert *et al.* (E598 Collaboration), Phys. Rev. Lett. **33,** 1404 (1974).

[3] G. Arnison *et al.* (UA1 Collaboration), Phys. Lett. **126B,** 398 (1983).

[4] P. Bagnaia *et al.* (UA2 Collaboration), Phys. Lett. **129B,** 130 (1983).

[5] M. Banner *et al.* (UA2 Collaboration), Phys. Lett. **122B,** 476 (1983).

[6] S. Chatrchyan *et al.* (CMS Collaboration), Phys. Lett. B **716,** 30 (2012).

[7] G. Aad *et al.* (ATLAS Collaboration), Phys. Lett. B **716,** 1 (2012).

[8] S. L. Glashow, Phys. Rev. **118,** 316 (1960).

[9] M. G. Aartsen *et al.* (IceCube Collaboration), Nature (London) **591,** 220 (2021); **592,** E11 (2021).

[10] L. A. Anchordoqui *et al.*, arXiv:2109.10905.

[11] E. A. Paschos and O. Lalakulich, arXiv:hep-ph/0206273.

[12] P. S. B. Dev and A. Soni, arXiv:2112.01424.

[13] H. Abreu *et al.* (FASER Collaboration), arXiv:2001.03073.

[14] B. Batell, J. L. Feng, A. Ismail, F. Kling, R. M. Abraham, and S. Trojanowski, Phys. Rev. D **104,** 035036 (2021).

[15] M. G. Aartsen *et al.* (IceCube Collaboration), J. Instrum. **12,** P03012 (2017).

[16] V. Barger, L. Fu, J. G. Learned, D. Marfatia, S. Pakvasa, and T. J. Weiler, Phys. Rev. D **90,** 121301 (2014).

[17] K. S. Babu, P. S. Dev, S. Jana, and Y. Sui, Phys. Rev. Lett. **124,** 041805 (2020).

[18] J. F. Donoghue, E. Golowich, and B. R. Holstein, *Dynamics of the Standard Model* (Cambridge University Press, Cambridge, England, 2014), Vol. 2.

[19] Q. Chang, X.-N. Li, X.-Q. Li, and F. Su, Chin. Phys. C **42,** 073102 (2018).

[20] K. Bondarenko, A. Boyarsky, D. Gorbunov, and O. Ruchayskiy, J. High Energy Phys. 11 (2018) 032.

[21] M. Passera, K. Philippides, and A. Sirlin, Phys. Rev. D **84,** 094030 (2011).

[22] A. Czarnecki, W. J. Marciano, and A. Sirlin, Phys. Rev. D **101,** 091301 (2020).

[23] F. Guerrero and A. Pich, Phys. Lett. B **412,** 382 (1997).

[24] M. G. Aartsen *et al.*, Nucl. Phys. B **908,** 161 (2016).

[25] H. Abreu *et al.* (FASER Collaboration), Eur. Phys. J. C **80,** 61 (2020).

[26] B. Batell, J. L. Feng, and S. Trojanowski, Phys. Rev. D **103,** 075023 (2021).

[27] P. A. Zyla *et al.* (Particle Data Group), Prog. Theor. Exp. Phys. **2020,** 083C01 (2020).

[28] T. Aoyama *et al.*, Phys. Rep. **887,** 1 (2020).

[29] G. W. Bennett *et al.* (Muon G-2 Collaboration), Phys. Rev. D **73,** 072003 (2006).

[30] B. Abi *et al.* (Muon g-2 Collaboration), Phys. Rev. Lett. **126,** 141801 (2021).

[31] C. Ahdida *et al.* (SHiP Collaboration), arXiv:2002.08722.

[32] H. Abreu *et al.* (FASER Collaboration), Phys. Rev. D **104,** L091101 (2021).

[33] R. Abbasi *et al.* (IceCube Collaboration), Astropart. Phys. **35,** 615 (2012).

[34] G. Apollinari, O. Brüning, T. Nakamoto, and L. Rossi, CERN Yellow Report No. CERN-2015-005, 2015, pp. 1–19.

[35] F. Juget, J. Phys. Conf. Ser. **160,** 012033 (2009).

[36] A. Ariga *et al.* (FASER Collaboration), arXiv:1812.09139.

[37] M. Przybycien, A. Szczurek, and G. Ingelman, Z. Phys. C **74,** 509 (1997).

[38] Liquid Argon Technology at BNL: Properties, https://lar.bnl .gov/properties/ (accessed: 2021-12-04).

[39] M. Honda, M. S. Athar, T. Kajita, K. Kasahara, and S. Midorikawa, Phys. Rev. D **92,** 023004 (2015).

[40] A. Ismail, R. Mammen Abraham, and F. Kling, Phys. Rev. D **103,** 056014 (2021).

[41] F. Kling and L. J. Nevay, Phys. Rev. D **104,** 113008 (2021).

[42] For reference, we expect fewer than 10^{-5} π^- events at FLArE-100 and FASERν2.

[43] While we assume that $\delta E/E \sim 5\%/(E/100 \text{ GeV})^{1/2}$ as presented in [35], Ref. [25] notes that a larger number of low-energy background electron tracks produced by high-energy muons may limit the energy resolution. We assume this is not the case; however this deserves further investigation.

[44] The spatial resolution in a LArTPC is limited by the wire spacing, of order 1 mm. We estimate the angular resolution as 1 mm/(track length).

[45] The $\bar{\nu}_e$ differential flux at 580 GeV, responsible for ρ^- resonant production, is $d\Phi_{\bar{\nu}_e}/dE_\nu \sim 5 \times 10^{-8}$ m^{-2} s^{-1} sr^{-1} GeV^{-1}. The atmospheric neutrino differential flux (all flavors) at 2.7 TeV is roughly $d\Phi_\nu/dE_\nu \sim 1 \times 10^{-8}$ m^{-2} s^{-1} sr^{-1} GeV^{-1} [39], approximately 5 times smaller than the relevant $\bar{\nu}_e$ flux. The neutral-current DIS cross section is given roughly by $\sigma_{\text{NC}}(\text{DIS}) \sim (E_\nu/2 \text{ TeV}) \times 10^{-35}$ cm^2 per nucleon [40], roughly 2 orders of magnitude larger than

that of ρ^- resonant production, $\sigma_{\mathrm{res}}(\rho^-) \sim 10^{-37} \mathrm{cm}^2$. Taking into account that there are roughly twice as many nucleons as electrons in water, this yields $S \colon B \sim 1 \colon 40$.

[46] Accounting for the slightly larger flux of ν_e relative to $\bar{\nu}_e$ and the fact that the cross section is twice as large,

we find an effective cross section of $\sigma_{\mathrm{eff}} \approx 3.5 \times \sigma_{\mathrm{DIS}}(\bar{\nu}_e) = 7 \times 10^{-36} \mathrm{\ cm}^2$ per nucleon, roughly 70 times larger than the resonant production cross section. Taking into account that there are roughly twice as many nucleons as electrons in water, this yields $S \colon B \sim 1 \colon 140$.